Available online at www.sciencedirect.com

SciVerse ScienceDirect

Journal of Nutritional Biochemistry 23 (2012) 1716–1724

Journal of Nutritional Biochemistry

Caveolin-3 is involved in the protection of resveratrol against high-fat-diet-induced insulin resistance by promoting GLUT4 translocation to the plasma membrane in skeletal muscle of ovariectomized rats

Zhi Tan[a,*,1], Li-Jun Zhou[a,1], Pan-Wei Mu[b], Shui-Ping Liu[c], Si-Juan Chen[a], Xiao-Dong Fu[a], Ting-Huai Wang[a,*]

[a]Department of Physiology, Zhongshan School of Medicine, Sun Yat-sen University, Guangzhou, P.R. China
[b]Department of Endocrinology, the Third Affiliated Hospital of Sun Yat-sen University, Guangzhou, P.R. China
[c]Department of Forensic Pathology, Zhongshan School of Medicine, Sun Yat-sen University, Guangzhou, P.R. China

Received 20 July 2011; received in revised form 28 November 2011; accepted 13 December 2011

Abstract

Insulin resistance is recognized as a common metabolic factor which predicts the future development of both type 2 diabetes and atherosclerotic disease. Resveratrol (RSV), an agonist of estrogen receptor (ER), is known to affect insulin sensitivity, but the mechanism is unclear. Evidence suggests that caveolin-3 (CAV-3), a member of the caveolin family, is involved in insulin-stimulated glucose uptake. Our recent work indicated that estrogen via ER improves glucose uptake by up-regulation of CAV-3 expression. Here, we investigated the role of CAV-3 in the effect of RSV on insulin resistance in skeletal muscle both *in vivo* and *in vitro*. The results demonstrated that RSV ameliorated high-fat-diet (HFD)-induced glucose intolerance and insulin resistance in ovariectomized rats. RSV elevated insulin-stimulated glucose uptake in isolated soleus muscle *in vivo* and in C2C12 myotubes *in vitro* by enhancing GLUT4 translocation to the plasma membrane rather than increasing GLUT4 protein expression. Through ERα-mediated transcription, RSV increased CAV-3 protein expression, which contributed to GLUT4 translocation. Moreover, after knockdown of CAV-3 gene, the effects of RSV on glucose uptake and the translocation of GLUT4 to the plasma membrane, as well as the association of CAV-3 and GLUT4 in the membrane, were significantly attenuated. Our findings demonstrated that RSV via ERα elevated CAV-3 expression and then enhanced GLUT4 translocation to the plasma membrane to promote glucose uptake in skeletal muscle, exerting its protective effects against HFD-induced insulin resistance. It suggests that this pathway could represent an effective therapeutic target to fight against insulin resistance syndrome induced by HFD.

Keywords: Insulin resistance; Caveolin-3; GLUT4; High-fat diet; Estrogen receptor

1. Introduction

Insulin resistance is recognized as the precursor to prediabetes and type 2 diabetes — an increased risk factor for cardiovascular diseases [1]. Reversing insulin resistance is an important way for the prevention of metabolic syndrome and heart disease. Epidemiological studies have demonstrated a decreased incidence in cardiovascular disorders among French populations, who adopt a diet containing high amounts of unsaturated fat acid largely due to the consumption of moderate amounts of red wine, a source of resveratrol (RSV) [2]. RSV, a phytoestrogen found naturally in grapes and red wine, is well recognized for its cardioprotective effects [3]. Recent investigations have revealed that RSV has the protective effects on diet-induced insulin resistance syndrome [4,5], but its molecular mechanisms remains unclear.

Insulin resistance can result in a decrease in glucose uptake in insulin-sensitive tissues, i.e., skeletal muscle and adipose tissues [6]. In these tissues, glucose uptake is mediated by one of the isoforms of the glucose transporter family, GLUT4. Incorporation of GLUT4-containing vesicles into the plasma membrane is a major rate-limiting step in determining insulin-stimulated glucose uptake [7,8]. Increasing evidence suggested that GLUT4 translocation to plasma membrane stimulated by insulin was enriched by caveolae [9–11]. Caveolae are flask-shaped membrane invaginations present in plasma membrane and may be distinguished by the presence of caveolins. Caveolin-3 (CAV-3), one isoform of caveolins, is predominantly expressed in skeletal muscle (for review, see Ref. [12]), which accounts for nearly 75% of total glucose disposal under insulin-stimulated conditions [13]. More importantly, different groups have demonstrated insulin resistance in the skeletal muscle of CAV-3 knockout mice [14,15], suggesting that CVA-3 may be a critical intermediate for glucose uptake. Our previous work has also shown that estrogen via its receptor improved glucose uptake by up-regulation of CAV-3

* Corresponding authors. Department of Physiology, Zhongshan School of Medicine, Sun Yat-sen University, Guangzhou 510080, P.R. China. Tel.: +86 20 87330647; fax: +86 20 87333232.
E-mail addresses: tanzhi@mail.sysu.edu.cn (Z. Tan), tinghuaiwang@yahoo.com (T.-H. Wang).
[1] Both authors contribute equally to this work.

0955-2863/$ - see front matter © 2012 Elsevier Inc. All rights reserved.
http://dx.doi.org/10.1016/j.jnutbio.2011.12.003

expression in skeletal muscle cells [16]. Numerous studies have shown that RSV has molecular structure and pharmacologic properties similar to those of estradiol, so it mimics many roles of estrogen (for review, see Ref. [17]). Therefore, we hypothesized that CAV-3 may be involved in the effects of RSV on insulin resistance.

In the present work, we first examined the effect of RSV on glucose homeostasis in high-fat diet (HFD) ovariectomized rats *in vivo* as well as in C2C12 myotubes *in vitro* stimulated by insulin. Then, we tested whether GLUT4 translocation to the plasma membrane was involved in this process mediated by RSV. The role of CAV-3 in RSV-induced changes was also evaluated.

2. Material and methods

2.1. Animals and experimental diets

Five-month-old female Sprague–Dawley rats were obtained from the Experimental Animal Center of Sun Yat-sen University (Guangzhou, China). Rats were separately housed in cages at 23°C±2°C under a 12-h light/dark cycle (lights on at 7:00 a.m.) and had free access to water and diet. After 1 week of acclimation, animals were subjected to a bilateral ovariectomy under ether anesthesia. And 3 weeks later, the rats were randomly divided into three groups fed with different diets for 16 weeks: (1) control diet group (CON), fed on chow diet; (2) high-fat-diet group (HFD), fed on HFD; (3) RSV intervention group (HFD+RSV), fed on HFD and RSV (10 mg/kg/day). Both diets were purchased from Experimental Animal Center of Sun Yat-sen University. On a caloric basis, the HF diet consisted of 60% fat, 28% carbohydrate and 12% protein (total 5.3 kcal/g), whereas the control diet contained 10% fat, 64% carbohydrate and 26% protein (total 3.9 kcal/g). The composition of the experimental diets is presented in Table 1. All animal procedures were approved by the Sun Yat-sen University Animal Care and Use Committee with NIH standards.

2.2. Preparation of blood and tissue samples and measurement of metabolic parameters

After 16 weeks of different diet feeding, rats were fasted overnight (16 h), and blood samples via tail vein were collected for the measurement of metabolic parameters. Fasting blood glucose was determined using Lifescan One-Touch Ultra Glucometer (Johnson & Johnson, USA). Fasting serum insulin was measured with an ultrasensitive rat insulin enzyme-linked immunosorbent assay kit (Mercodia AB, Uppsala, Sweden) according to the manufacturer's instruction. The value of the homeostasis model assessment of insulin resistance (HOMA-IR) index was calculated by using insulin and glucose values in fasting condition. Then, an intraperitoneal glucose tolerance test (IPGTT) was conducted by intraperitoneal injection of glucose solution at 2 g/kg body weight, and blood glucose was measured at 0, 15, 30, 60, 90 and 120 min postinjection. Lastly, soleus muscles were isolated from the three different groups, and basal and insulin-stimulated skeletal muscle glucose uptakes were measured.

Table 1
Composition of experimental diets

Macronutrient	CON		HFD	
	g %	kcal %	g %	kcal %
Protein	25.3	26	15.7	12
Carbohydrate	62	64	36.7	28
Fat	4.31	10	35	60
Total	91.6	100	87.5	100
Kcal/g	3.9		5.3	
Ingredients	g	kcal	g	kcal
Casein	260	1040	120	480
L-Cystine	3.9	12	1.8	7.2
Cellulose	50	0	50	0
Corn starch	402	1610	39.2	156.8
Maltodextrin 10	135	540	125	500
Sucrose	100	400	110	440
Soybean oil	25	225	25	225
Lard	20	179.6	246	2211
t-Butylhydroquinone	0.01	0	0	0
Mineral mix	35	0	10	0
Dicalcium phosphate	0	0	13	0
Calcium carbonate	0	0	5.5	0
Potassium citrate	0	0	16.5	0
Vitamin mix	10	40	10	40
Choline bitartrate	2.5	0	2	0
Total	1044	4046	774	4060

2.3. Uptake of 2-deoxy-[^{3}H] glucose

Tissue-specific glucose uptake was measured by D-[^{3}H] glucose described by Oshikawa et al. [15]. Briefly, soleus skeletal muscles were dissected out and rapidly cut into pieces. Next, muscle tissues were seeded into 12-well culture plate containing 2 ml Krebs–Ringer bicarbonate (KRB) buffer (pH 7.4, 8 mmol/L glucose) and incubated at 37°C for 60 min. Afterward, the muscle tissues were incubated for 30 min in KRB buffer in the presence (for measurement of insulin-stimulated glucose uptake) or absence (for measurement of basal glucose uptake) of 100 nM insulin. Tissues were then rinsed using KRB buffer and further incubated for 30 min at 37°C in 2 ml KRB buffer containing 1 μCi 2-deoxy-[^{3}H] glucose. Plates were supplied continuously with 95% O_2/5% CO_2 throughout the experiment, and insulin was present during the wash and for measuring insulin-stimulated glucose uptake. Tissues were then removed, rapidly rinsed in isotope-free KRB buffer and solubilized with 1 N NaOH. Radioactivity was counted using liquid scintillation counter. Results were expressed as counts per minute of 2-deoxy-[^{3}H] glucose uptake per 10 mg tissue.

At the cell level, C2C12 myotubes were incubated in 12-well cluster dishes, washed twice with phosphate-buffered saline (PBS) and incubated in serum-free media for 16 h and then treated with or without 10^{-5} M RSV in Dulbecco's modified Eagle's medium for 24 h at 37°C. Cells were incubated in 2 ml of KRH (25 mM HEPES, 120 mM NaCl, 5 mM KCl, 1.2 mM $MgSO_4$, 1.3 mM $CaCl_2$ and 1.3 mM KH_2PO4) with 100 nM insulin for 20 min. 2-Deoxy-[^{3}H] glucose (1 μCi) was added to each well for 10 min. Cells were washed with KRH buffer twice and then lysed in 1 N NaOH. Glucose uptake values were corrected for non-carrier-mediated transport by measuring glucose uptake in the presence of 10 mM cytochalasin B (Sigma, St. Louis, MO, USA). In some experiments, cells were preincubated with (PPT; 10^{-6} M, an ERα-selective agonist, Sigma, St. Louis, MO, USA), methyl-piperidino-pyrazole (MPP; 10^{-6} M, an ERα-selective antagonist, Sigma), 2,3-bis(4-hydroxyphenyl)propionitrile (DPN; 10^{-6} M, an ERβ-selective agonist, Sigma) and 1-(4-(6-bromobenzo[1,3]dioxol-5-yl)-3a,4,5,9b-tetrahydro-3H-cyclopenta[c]quinolin-8-yl)-ethanone (G-1; 10^{-6} M, a selective GPR30 agonist, Sigma) for 30 min at 37°C before treatment with or without RSV (10^{-5} M).

2.4. Western blot analysis

Whole cell lysates or plasma membrane fractions were separated on 10% sodium dodecyl sulfate polyacrylamide gel electrophoresis (SDS-PAGE) and transferred to polyvinylidene fluoride membrane (Amersham) in the Tris–glycine buffer containing 20% methanol. Membranes were washed with tris-buffered saline Tween-20 (TBST), blocked with 10% skim milk for 1 h and incubated with the primary antibodies (CAV-3, GLUT4 and β-actin) at the dilution recommended by the manufacturer (Santa Cruz). Membranes were washed in TBST buffer, probed with horseradish-peroxidase-conjugated secondary antibodies (goat anti-rabbit or goat anti-mouse IgG) and visualized using the enhanced chemiluminescence kit (Amersham). Densitometric analysis was performed using the densitometer (Gel Doc, Bio-Rad) to quantify protein expression levels.

2.5. C2C12 myotubes culture and immunocytochemistry

C2C12 myoblasts were maintained in Dulbecco's modified Eagle's medium supplemented with 10% fetal bovine serum at 37°C in a 5% CO_2–95% air incubator. When 70% confluency was reached, the cells were transfected with the CAV-3 siRNA constructs or scramble siRNA used as control (Santa Cruz) using Lipofectamine 2000 (Invitrogen) according to the manufacturer's instructions, and 1 day later, the medium was replaced with Dulbecco's modified Eagle's medium containing 1% fetal bovine serum for 3 days. After 7 days of differentiation, the cultures were fixed and stained with antibodies against CAV-3 and GLUT4 to characterize the expression of CAV-3 and GLUT4. Briefly, cells were washed with cold PBS three times, fixed with cold methanol and kept at −20°C for 15 min. After rinsing with PBS, cultures were preincubated in 3% bovine serum albumin (BSA) for 30 min. Then, cells were incubated with primary antibodies: mouse monoclonal anti-CAV-3 (1:500; Santa Cruz Biotechnology, CA, USA) and rabbit polyclonal anti-GLUT4 (1:500; Santa Cruz Biotechnology) in 3% BSA with 0.1% Triton X-100 dissolved in PBS for 1 h at room temperature. After washing three times with PBS for 10 min, cells were incubated with goat anti-mouse tetramethyl rhodamine isothiocyanate (TRITC; 1:500; Sigma, St. Louis, MO, USA) or goat anti-rabbit fluorescein isothiocyanate (FITC)-conjugated antibody (1:500; Jackson Immuno Research, PA, USA) for 1 h in the dark.

The immunofluorescence cells were visualized using a confocal laser-scanning microscope (LSM 710, Zeiss, Germany). The fluorophores FITC and TRITC were excited by the 488 -and 543-nm laser lines, respectively, followed by emission collection with a 505–530-nm band pass and a 560–615-nm band pass filter, respectively. The thickness of each optical slice was 0.6 μm, and confocal *z*-stack images were taken through the depth of the cells at intervals of 0.8 μm.

If both red and green signals were expressed in the same place, this resulted in a yellow signal. An average percentage of the area of the yellow signal (showing colocatization) relative to the total area of a whole cell was collected using identical acquisition parameters and analyzed by a computerized image analysis system (Image-Pro Plus 5.0; Media Cybernetics, USA), and then the mean±S.E. value across the different groups was determined. Five cells were included for each group for

quantification of the results of immunocytochemistry. Quantitative analyses of immunofluorescence staining were conducted in a blinded manner.

2.6. Plasma membrane isolation

Plasma membrane isolation was performed according to the manufacturer's instruction (Calbiochem). Briefly, for C2C12 myotubes, after carefully removing Wash Buffer, add a mixture of Protease Inhibitor Cocktail and cold Extraction Buffer I (1:200) to a flask. Incubate for 10 min at 4°C under gentle agitation. Discard the supernatant, and make sure that all liquid is removed. Add a mixture of Protease Inhibitor Cocktail and cold Extraction Buffer II (1:200) again and incubate for 30 min at 4°C under gentle agitation. Keep the supernatant (membrane fractions enriched in integral membrane and membrane associated proteins). For skeletal tissue, quickly remove unwanted materials at 4°C, slice it in ~2 mm^3 pieces, and transfer into a tube containing 2 ml ice-cold Wash Buffer. Gently flick the tube a few times to rinse off blood cells and other loosely attached substances. Centrifuge tissue pieces at 100*g* and 4°C for 2 min. Carefully remove the supernatant, add another 2 ml ice-cold Wash Buffer, and repeat washing steps. After the final washing step, take care to completely remove all buffers. Protein concentration was determined using the Bradford method.

2.7. Immunoprecipitation

For immunoprecipitation, 200 μg of cellular protein was incubated with 1 μg of CAV-3 overnight at 4°C. Twenty microliters of protein A/G plus-agarose (Santa Cruz) was added to each sample and incubated for 4 h. Immunocomplexes were collected and washed with lysis buffer three times. The samples were boiled for 3 min, and the beads were removed by centrifugation. Proteins were separated by 7.5% SDS-PAGE and transferred to a nitrocellulose membrane. The blots were blocked with 10% milk solution in TBST buffer, incubated with GLUT4 antibodies in TBST and then incubated with secondary antibodies conjugated to horseradish peroxidase. The immunoreactive bands were visualized by enhanced chemiluminescence.

2.8. Real-time polymerase chain reaction (PCR)

Total RNAs were isolated using Trizol (Invitrogen) according to the manufacturer's instruction. PCR was performed on the ABI Prism 7000 using One Step SYBR PrimeScript RT-PCR Kit (TaKaRa, Shanghai). The following primers were used: CAV-3, sense ACACCACTTTCACCGTCTCCAAGT, antisense TGTGGCAGAAGGAGATACAGGCAA; β-actin, sense AGCCATGTACGTAGCCATCC, antisense CTCTCAGCTGTGGTGGTGAA. Data were collected in the extension step. The specificity and identity of PCR products were verified using melting curve analysis following the PCR, which distinguished specific PCR products from the primer dimmer-caused nonspecific PCR. Results were analyzed using the software provided by the manufacturer.

2.9. Statistical analysis

Data were expressed as means±S.E., and analysis of variance was performed using SPSS 13.0 software. Data between experimental and control groups were evaluated by one-way analysis of variance to determine specific mean differences, and the comparison of mean values between the groups was determined by Student–Newman–Keuls test. Statistical significance was considered as a P value <.05.

3. Result

3.1. RSV exerted a protective effect against HFD-induced glucose and insulin intolerance

As shown in Fig. 1, after 16 weeks of diet exposure, fasting serum glucose and fasting insulin concentrations in HFD group increased significantly compared with those in the CON group, but supplementation of RSV evidently inhibited the increase of serum glucose and

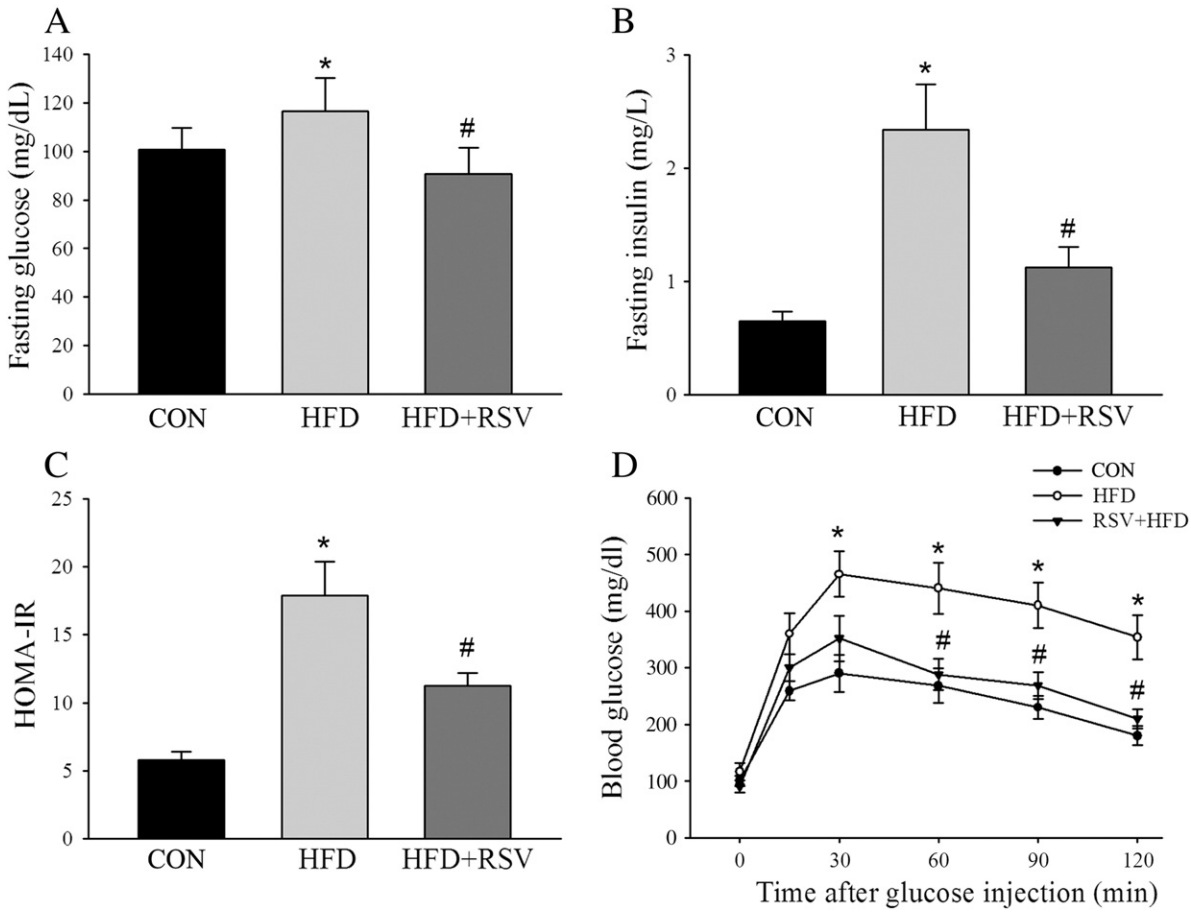

Fig. 1. RSV protects against HFD-induced insulin resistance in ovariectomized rats. (A–C) At the end of the different 16-week diets, rats were fasted overnight, and fasting blood glucose (A), fasting serum insulin (B) and HOMA-IR values (C) were measured. (D) An IPGTT was then performed at time 0, 15, 30, 60, 90 and 120 min after injection with glucose load (ip 2 g/kg body wt). Values are expressed as means±S.E. Six to eight rats were analyzed in each group. CON: the control chow diet group; HFD: the high-fat diet group; HFD+RSV: the high-fat diet supplemented with RSV group. *P<.05 vs. CON; #P<.05 vs. HFD.

insulin concentrations ($P<.05$ vs. HFD alone, Fig. 1A and B). In addition, HOMA-IR was significantly higher in the HFD group than in the control diet group, while lower HOMA-IR was seen in the RSV-treatment group ($P<.05$ vs. HFD group, Fig. 1C). An IPGTT was performed to assess whole body glucose clearance in response to a glucose challenge. HFD resulted in a higher blood glucose levels and a larger decline in whole body glucose tolerance, as demonstrated by the inability of HFD rats to effectively clear glucose from their blood by the end of the 2-h test compared to CON (Fig. 1D). However, glucose tolerance was improved in the third group supplied with RSV. At 30, 60, 90 and 120 min after glucose injection, the blood glucose levels were lower in the third group than in the HFD group ($P<.05$ vs. HFD). These results indicated that supplementation of RSV ameliorated HFD-induced glucose and insulin intolerance in rats with bilateral ovariectomy.

3.2. RSV directly enhances insulin-stimulated glucose uptake in an ERα-dependent manner

We next explored the effect of RSV administration on glucose uptake in isolated soleus muscle and C2C12 myotubes. As shown in Fig. 2A, our data demonstrated that the basal glucose uptake in the soleus muscles was not significantly different among groups. As expected, HFD caused a remarkable decrease in insulin-stimulated glucose uptake in skeletal muscle, whereas this was fully restored by the addition of RSV, indicating that RSV promoted skeletal muscle glucose uptake.

Subsequently, we used different agonist or antagonist of ER to investigate which ER subtype played a role in the promotion of glucose uptake mediated by RSV in C2C12 myotubes. As shown in Fig. 2B, RSV alone can also increase the glucose uptake, but it demonstrated a relatively lower potential of increasing glucose uptake compared with insulin-stimulated or insulin plus RSV. Accordingly, we focused on insulin-stimulated glucose in the following experiments. Only PPT significantly augmented and MPP significantly inhibited the insulin-stimulated glucose uptake, whereas

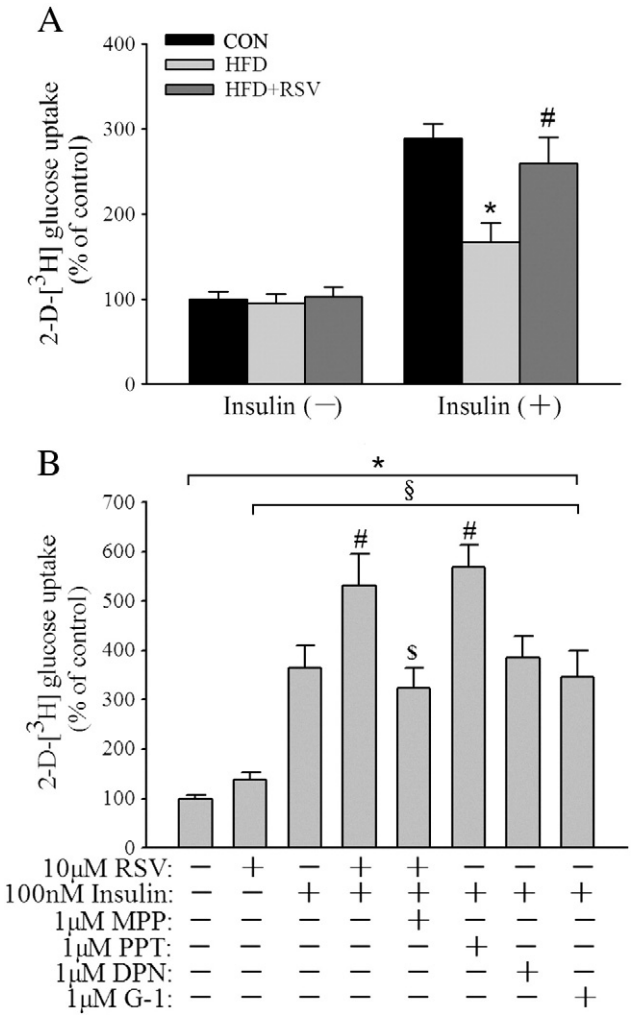

Fig. 2. RSV promotes glucose uptake mediated by ERα. (A) After 16 weeks of diet feeding, soleus muscles were isolated from the three different groups and used to measure 2-deoxy-[3H] glucose uptake. *$P<.05$ vs. CON; #$P<.05$ vs. HFD. (B) Different agonist or antagonist of ER was employed to investigate the ER subtype mediating the promotion of RSV on glucose uptake in C2C12 myotubes. *$P<.05$ vs. basal condition; §$P<.05$ vs. RSV alone; #$P<.05$ vs. insulin alone; $$P<.05$ vs. RSV plus insulin.

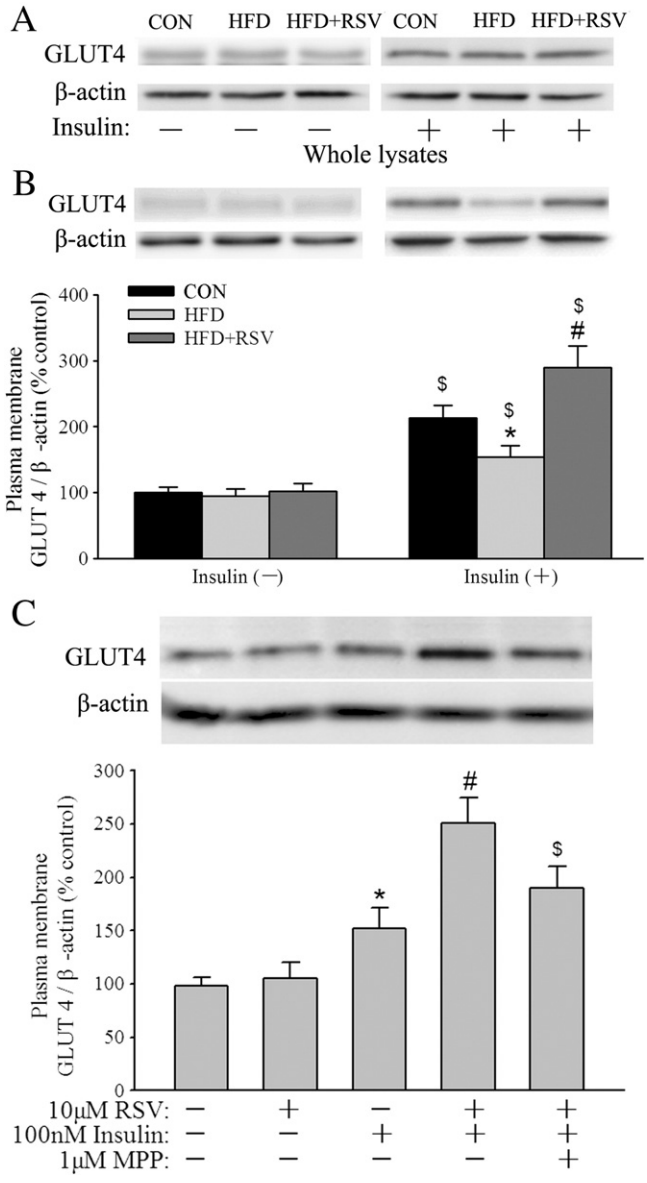

Fig. 3. RSV enhances GLUT4 translocation to plasma membrane in an ERα-dependent manner. (A, B) Effects of RSV on GLUT4 protein expression in whole tissue lysates (A) or in plasma membrane fractions (B) under basal or insulin-stimulated conditions. *$P<.05$ vs. CON; #$P<.05$ vs. HFD. (C) Pretreatment with ERα-selective antagonist MPP significantly inhibited the enhancement of RSV on GLUT4 translocation in C2C12 myotubes. *$P<.05$ vs. basal condition or RSV alone; #$P<.05$ vs. insulin alone; $$P<.05$ vs. RSV plus insulin.

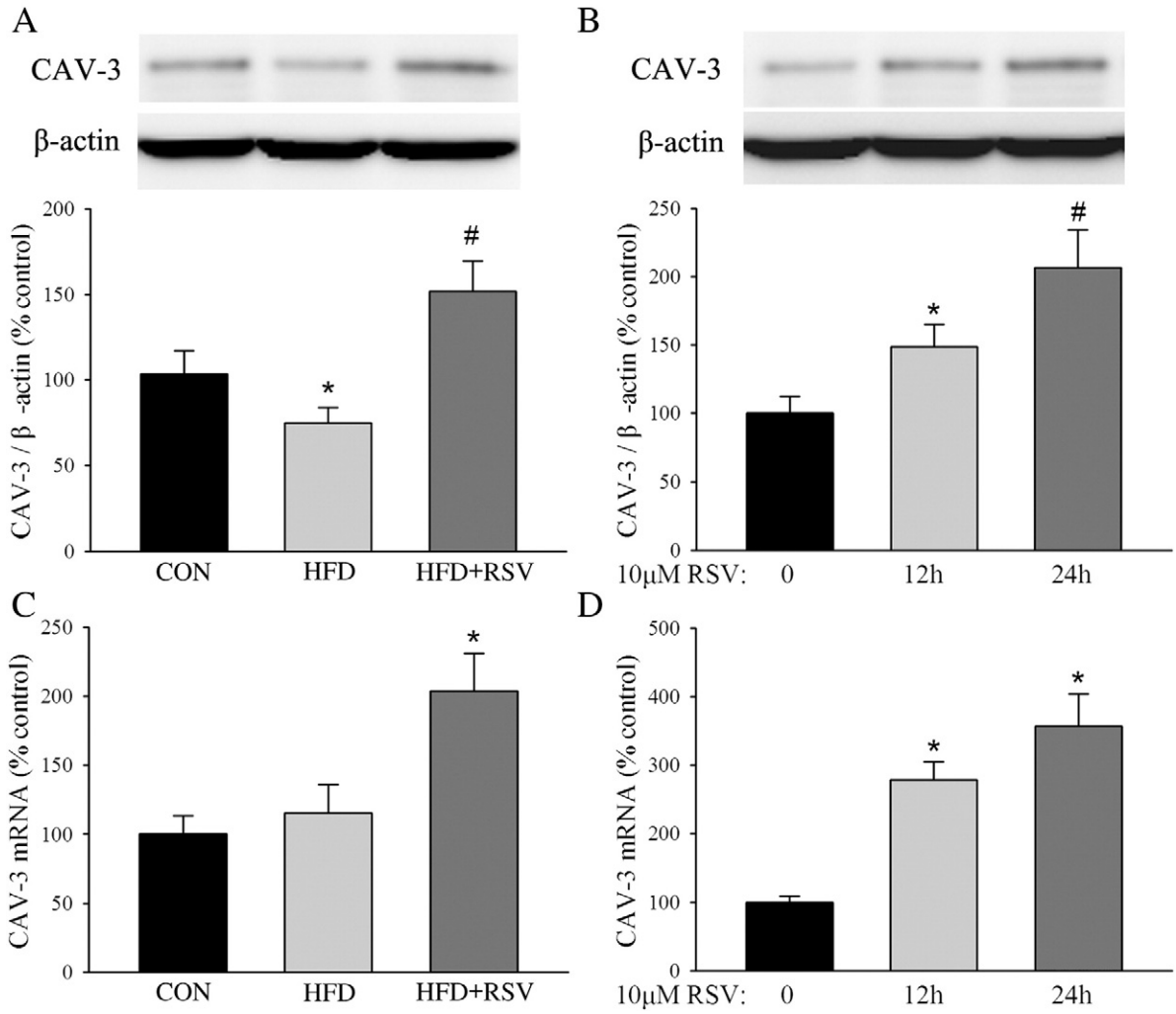

Fig. 4. RSV up-regulates CAV-3 expression in HFD-induced insulin-resistant soleus muscles and in C2C12 myotubes. (A, C) CAV-3 protein expression or mRNA levels were measured in soleus skeletal muscles isolated from CON, HFD or HFD supplied with RSV groups after 16 weeks of different diets. *P<.05 vs. CON; #P<.05 vs. HFD. (B, D) The changes of CAV-3 protein expression or mRNA levels were determined in C2C12 myotubes incubated with RSV for 12 h or 24 h (10^{-5} M). *P<.05 vs. basal condition; #P<.05 vs. treatment with RSV for 12 h.

DPN and G-1 had no effect on the insulin-stimulated glucose uptake. The results showed that ERα was related to the promotion of RSV on glucose uptake in skeletal muscle.

3.3. RSV enhanced GLUT4 translocation to the plasma membrane in an ERα-dependent manner

Insulin-stimulated uptake of glucose and the maintenance of glucose homeostasis are primarily mediated by mobilizing GLUT4 glucose transporters from intracellular membrane storage sites to the plasma membrane [18]. So, we next examined the effect of RSV treatment on the expression of GLUT4 protein in skeletal muscle and C2C12 skeletal muscle myotubes stimulated by insulin. As shown in Fig. 3A, total GLUT4 content in soleus muscles was unchanged among different diet groups in the absence or presence of insulin. However, under insulin-stimulated conditions, the plasma membrane GLUT4 protein concentration was evidently higher compared to the content under the basal conditions between all groups. Furthermore, insulin-stimulated plasma membrane GLUT4 protein level was lower in soleus muscles with intake of HFD for 16 weeks, while RSV supplement markedly reversed the effect (P<.05, Fig. 3B), suggesting that treatment with RSV affected GLUT4 translocation to plasma membrane rather than GLUT4 expression.

We next explored the role of ERα in the effect of RSV on GLUT4 translocation in C2C12 myotubes in the same manner. With or without pretreatment with MPP (10^{-6} M) for 30 min before, C2C12 myotubes were incubated with RSV (10^{-5} M) for an additional 24 h and then stimulated by insulin (100 nM) for 10 min. In Fig. 3C, insulin stimulation increased plasma membrane GLUT4 protein concentration above basal levels. Ten micromolars of RSV alone had no apparent effect under basal conditions, but enhanced insulin-stimulated plasma membrane GLUT4 protein concentration. Furthermore, pretreatment with ERα-selective antagonist MPP apparently inhibited the effect of RSV. Therefore, our results indicated that

Fig. 5. CAV-3 siRNA inhibits the promoting effect of RSV on glucose uptake and GLUT4 translocation. (A) Western blot showed the efficient inhibition of CAV-3 siRNA on CAV-3 protein expression. (B–D) C2C12 myotubes were transfected with CAV-3 siRNA or scramble siRNA for 24 h, followed by treatment with RSV (10^{-5} M) for 24 h and stimulation by insulin (100 nM) for 10 min, and then were prepared for the following experiments: (B) 2-deoxy-[^{3}H] glucose uptake; (C) Western blot analysis of GLUT4 protein levels; (D) immunoprecipitation to assess the possibility of interactions between CAV-3 and GLUT4. *P<.05 vs. control; #P<.05 vs. RSV plus insulin treatment. (E) Immunofluorescence staining to identify the expression of CAV-3 (red) and GLUT4 (green). The yellow signals indicate the colocalization of CAV-3 and GLUT4 in the same cell. Scale bar=10 μm. (F) The histogram indicated that the proportion of the colocalization of CAV-3 and GLUT4 in the total whole cell was changed between scramble siRNA and CAV-3 siRNA group. *P<.05 vs. scramble siRNA.

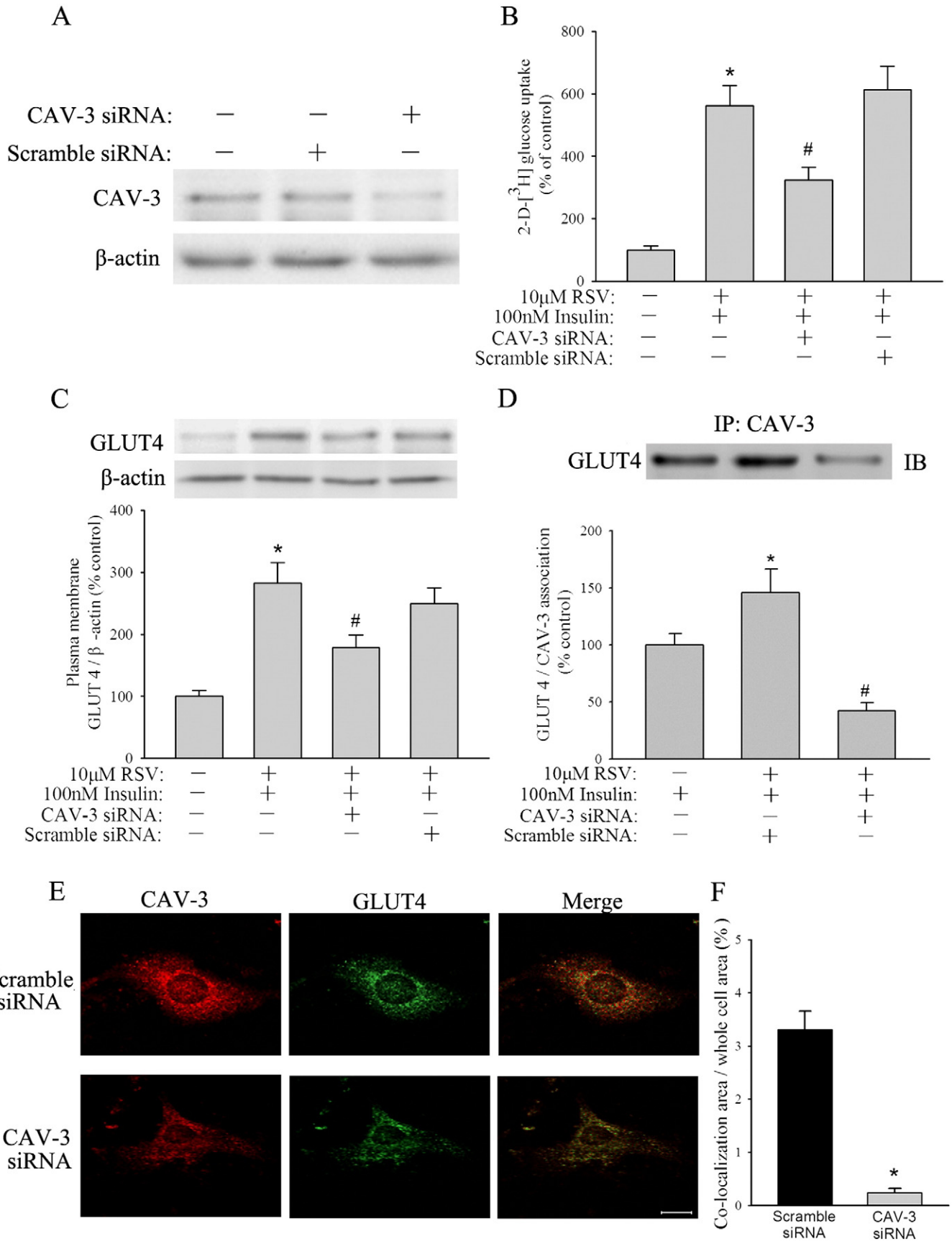
A
CAV-3 siRNA: − − +
Scramble siRNA: − + −
CAV-3
β-actin
B
2-D-[3H] glucose uptake (% of control)
800
600
400
200
0
*
#
10μM RSV: − + + +
100nM Insulin: − + + +
CAV-3 siRNA: − − + −
Scramble siRNA: − − − +
C
GLUT4
β-actin
Plasma membrane GLUT 4 / β -actin (% control)
400
300
200
100
0
*
#
10μM RSV: − + + +
100nM Insulin: − + + +
CAV-3 siRNA: − − + −
Scramble siRNA: − − − +
D
IP: CAV-3
GLUT4
IB
GLUT 4 / CAV-3 association (% control)
200
150
100
50
0
*
#
10μM RSV: − + +
100nM Insulin: + + +
CAV-3 siRNA: − − +
Scramble siRNA: − + −
E
CAV-3
GLUT4
Merge
Scramble siRNA
CAV-3 siRNA
F
Co-localization area / whole cell area (%)
5
4
3
2
1
0
*
Scramble siRNA
CAV-3 siRNA

RSV enhanced GLUT4 translocation to plasma membrane in an ERα-dependent manner.

3.4. RSV increases CAV-3 expression in HFD-induced insulin resistant soleus muscles and in C2C12 myotubes

It is reported that CAV-3 plays an important role in the regulation of glucose homeostasis *in vivo* as well as the development of insulin resistance [14]. To investigate whether CAV-3 was involved in the protection of RSV against HFD-induced insulin intolerance, we first employed Western blot and real-time PCR to examine the change of CAV-3 expression after RVS application in HFD-induced insulin-resistant soleus muscles and in C2C12 myotubes. As shown in Fig. 4, RSV not only affected CAV-3 protein expression but also resulted in an increase of mRNA levels in both soleus skeletal muscles isolated from HFD supplied with RSV group and C2C12 myotubes incubated with RSV for 12 h or 24 h. These results indicated that RSV up-regulated CAV-3 expression at the levels of transcription.

3.5. CAV-3 facilities RSV-induced glucose uptake and GLUT4 plasma membrane translocation

To further elucidate the role of CAV-3 in the salutary effect of RSV on insulin intolerance, we used CAV-3 siRNA to study its effect on GLUT4 translocation to plasma membrane in C2C12 myotubes. The down-regulation of CAV-3 by siRNA was confirmed by Western blot analysis of the inhibition of intracellular CAV-3 (Fig. 5A). As shown in Fig. 5B–C, we found that CAV-3 siRNA evidently reduced RSV-induced glucose uptake and GLUT4 translocation, but scramble siRNA had no effect ($P<.05$). We used immunoprecipitation to assess the possibility of interactions between CAV-3 and GLUT4 in the membrane of C2C12 myotubes. Compared with scramble siRNA control, CAV-3 siRNA significantly blocked RSV-induced association of CAV-3 and GLUT4 in the membrane of C2C12 myotubes stimulated by insulin (Fig. 5D). As show in Fig. 5E, the yellow signal in double immunofluorescence staining showed that GLUT4 (green) was colocalized with CAV-3 (red). Statistical analysis of the result showed that the proportion of the colocalization of CAV-3 and GLUT4 in the total whole cell was significantly lower in the CAV-3 siRNA-treated group (Fig. 5F, 3.31%±2.82%, $P<.05$ vs. 0.24%±0.02%, scramble siRNA group, $n=5$). Taken together, our data suggested that CAV-3 was involved in the RSV stimulation of glucose uptake and GLUT4 translocation to the plasma membrane.

4. Discussion

The present study demonstrated that RSV promoted glucose uptake in isolated soleus muscle and in C2C12 myotubes stimulated by insulin and ameliorated HFD-induced glucose and insulin intolerance in ovariectomized rats. RSV promotion of glucose uptake was related to enhancing GLUT4 translocation to plasma membrane rather than increasing GLUT4 protein expression. Moreover, after CAV-3 knockdown, the promoting effects of RSV on glucose uptake, GLUT4 translocation to the plasma membrane and the association of CAV-3 and GLUT4 in the membrane were significantly attenuated. The major finding of the present study was that RSV via ERα elevated CAV-3 expression to promote GLUT4 translocation to the plasma membrane and then facilitated glucose uptake in skeletal muscle, which contributed to its protection in HFD-induced insulin resistance.

Insulin resistance is one of the major features of the metabolic syndrome [19,20]. To date, all animal studies on insulin resistance have been conducted in monkeys, rats or transgenic mice fed with a normal chow or a moderately HFD, an unhealthy diet contributing to a growing worldwide incidence of type 2 diabetes and cardiovascular diseases [21]. Data from several research groups have demonstrated that postmenopausal women, as compared to premenopausal women, have increased fasting insulin [22,23] and increased fasting glucose levels [24], indicating a worsened insulin sensitivity after menopause. It was reported that ovariectomy, usually used to investigate the mechanisms responsible for menopause-related complications, could result in glucose intolerance and insulin resistance by induced estrogen deficiency [25]. Recent *in vitro* and *in vivo* studies have shown that RSV can affect insulin sensitivity and have antidiabetic properties [15,26,27], but the exact mechanism is largely unknown until now. It is well known that RSV is classified as a phytoestrogen due to its ability to interact with ER and its molecular structure pharmacologic properties similar to those of estrogen, so it mimics many roles of estrogen (for review, see Ref. [17]). Estrogen is recognized as an important regulator of insulin sensitivity and glucose tolerance [28–30]. Several recent studies found that post-menopausal women with an HFD lifestyle, when randomized to estrogen therapy, had a 35% lower risk of developing diabetes compared to placebo-treated women [15,31]. So, in the present study, we used ovariectomized rats to explore the effects of RSV and its mechanism of regulation of glucose uptake and insulin resistance for the first time. Our founding exhibited that RSV supplementation to ovariectomized rats inhibited the increase of serum glucose and insulin concentrations, suggesting that RSV could attenuate the development of insulin resistance. This finding is consistent with previous studies showing that RSV improves insulin sensitivity in type 2 diabetes patients [26] and in rats fed a high-cholesterol–fructose diet [5]. Therefore, the effects of RSV on glucose metabolism are of clinical importance to treat subjects with type 2 diabetes, especially in the postmenopausal women with HFD.

RSV is considered as one of the phytoestrogens which can induce transcriptional activity of ER [32], although Deng and his colleagues [5] have reported that ER is a key regulator in RSV-stimulating insulin-dependent glucose uptake, which accounts for the protective effects of RSV on diet-induced insulin resistance syndrome. They used pure ER antagonist ICI 182780 rather than a specific agonist or antagonist of ER to investigate the role of ER in the protection of RSV in glucose homeostasis. In addition, recent investigations have revealed that G-protein-coupled receptor 30 (GPR30) is one type of ER [33]. Consequently, it is still not known which subtype or subtypes of ERs mediate the action of RSV in this process. In the present study, we utilized specific agonist or antagonist of ERs to demonstrate that ERα mediated the desirable effects of RSV on glucose homeostasis. However, ERβ and GPR30 had no contribution to the effect of RSV. This result is consistent with the reported result from Riant et al. who used ERα knockout mice to demonstrate that ERα mediated the protection of estrogens against HFD-induced glucose intolerance [34]. Although a study showed that RSV binds ERβ and ERα with comparable affinity [17], a recent study from Gorres et al. demonstrated that HFD induced decreased expression of ERβ without altering insulin-stimulated glucose transport in soleus muscles [35], which further confirms that ERβ is not involved in the favorable effects on glucose homeostasis mediated by RSV.

Based on the above studies, we have demonstrated that RSV through ERα to promotion glucose uptake in skeletal muscle which contribution to ameliorate glucose intolerance. Insulin regulates the uptake of glucose into skeletal muscle by enhancing GLUT4 translocation to plasma membrane. This process is important for the regulation of glucose homeostasis. Our results showed that RSV treatment promoted GLUT4 translocation to the plasma membrane, but had no effect on total GLUT4 expression in skeletal muscle.

Caveolins are membrane proteins, the major coat proteins of caveolae and specialized lipid rafts in the plasma membrane that serve as scaffolding sites for many signaling complexes, such as insulin signaling [36,37]. Insulin increases GLUT4 to plasma

membrane fraction enriched by caveolae [9,38]. Our recent study has demonstrated that estrogen via its receptor improves glucose uptake by the up-regulation of CAV-3 expression in skeletal muscle cells [16]. In the present work, we showed that RSV up-regulated CAV-3 expression in HFD-induced insulin-resistant soleus muscles and in C2C12 myotubes. To confirm whether CAV-3 plays a role in RSV-induced promotion of insulin-stimulated glucose uptake, we used siRNA technology for the knockdown of CAV-3 protein expression to examine this effect. As expected, CAV-3 siRNA significantly blocked the promotion of glucose uptake mediated by RSV. These findings indicated that CAV-3 is involved in RSV-mediated glucose uptake. A previous study indicated that CAV-3 had a role in the GLUT4 translocation in conditionally immortalized skeletal muscle cells [39]. A recent study also showed that RSV could increase the association between CAV-3 and GLUT4 in diabetic myocardium [4]. To further confirm the role of CAV-3 in the action of RSV on GLUT4 translocation, we used immunoprecipitation and immunofluorescence to investigate the effect of CAV-3 on GLUT4 translocation stimulated by insulin in C2C12 myotubes. Our results demonstrated that knockdown of CAV-3 significantly suppressed RSV-induced association of CAV-3 and GLUT4 in the membrane of C2C12 myotubes stimulated by insulin, which was similar to the effect of RSV on glucose uptake. However, our results were not consistent with a previous study demonstrating that CAV-1 rather than CAV-3 played an important role in glucose uptake in differentiated muscle cells [40]. This discrepancy may be interpreted by the different methods of treatment of cells used in the experiments. Taken together, our current study demonstrated that CAV-3 played a crucial role in the RSV protection against HFD-induced insulin resistance through a direct interaction with GLUT4 translocation to the plasma membrane, which was consistent with previous works. And the role of CAV-3 in GLUT4 translocation was also confirmed in a recent study, demonstrating that translocation of caveolin-3 and GLUT4 to caveolae resulted in delayed protection in the myocardium [41].

In conclusion, our results indicated that RSV could ameliorate insulin resistance in skeletal muscle by enhancing glucose uptake through a CAV-3-dependent pathway. The protection of RSV is mainly mediated in an ERα-dependent manner to up-regulate CAV-3 protein expression, subsequently leading to the enhancement of GLUT4 translocation to plasma membrane, which might account for the beneficial effect of RSV on insulin resistance. It provided a novel strategy for pharmaceutical intervention that targeting CAV-3 in RSV-mediated signaling pathway on insulin resistance may produce therapeutic effects for menopausal women with type 2 diabetes.

Acknowledgments

This work was supported by a grant from Sun Yat-sen University Summer Student Investigation (2011-SUM-07), the National Natural Science Foundation of China (no. 31000489) and a grant from the Department of Science and Technology in Guangdong province of China (2010B031600049).

References

[1] Reaven GM. Pathophysiology of insulin resistance in human disease. Physiol Rev 1995;75:473–86.
[2] Renaud S, de Lorgeril M. Wine, alcohol, platelets, and the French paradox for coronary heart disease. Lancet 1992;339:1523–6.
[3] Petrovski G, Gurusamy N, Das DK. Resveratrol in cardiovascular health and disease. Ann N Y Acad Sci 2011;1215:22–33.
[4] Penumathsa SV, Thirunavukkarasu M, Zhan L, Maulik G, Menon VP, Bagchi D, et al. Resveratrol enhances GLUT-4 translocation to the caveolar lipid raft fractions through AMPK/Akt/eNOS signalling pathway in diabetic myocardium. J Cell Mol Med 2008;12:2350–61.
[5] Deng JY, Hsieh PS, Huang JP, Lu LS, Hung LM. Activation of estrogen receptor is crucial for resveratrol-stimulating muscular glucose uptake via both insulin-dependent and -independent pathways. Diabetes 2008;57:1814–23.
[6] Bell GI, Polonsky KS. Diabetes mellitus and genetically programmed defects in beta-cell function. Nature 2001;414:788–91.
[7] Rea S, James DE. Moving GLUT4: the biogenesis and trafficking of GLUT4 storage vesicles. Diabetes 1997;46:1667–77.
[8] Thurmond DC, Pessin JE. Discrimination of GLUT4 vesicle trafficking from fusion using a temperature-sensitive Munc18c mutant. EMBO J 2000;19:3565–75.
[9] Gustavsson J, Parpal S, Stralfors P. Insulin-stimulated glucose uptake involves the transition of glucose transporters to a caveolae-rich fraction within the plasma membrane: implications for type II diabetes. Mol Med 1996;2:367–72.
[10] Cohen AW, Combs TP, Scherer PE, Lisanti MP. Role of caveolin and caveolae in insulin signaling and diabetes. Am J Physiol Endocrinol Metab 2003;285:E1151–60.
[11] Karlsson M, Thorn H, Parpal S, Stralfors P, Gustavsson J. Insulin induces translocation of glucose transporter GLUT4 to plasma membrane caveolae in adipocytes. FASEB J 2002;16:249–51.
[12] Cohen AW, Hnasko R, Schubert W, Lisanti MP. Role of caveolae and caveolins in health and disease. Physiol Rev 2004;84:1341–79.
[13] DeFronzo RA, Jacot E, Jequier E, Maeder E, Wahren J, Felber JP. The effect of insulin on the disposal of intravenous glucose. Results from indirect calorimetry and hepatic and femoral venous catheterization. Diabetes 1981;30:1000–7.
[14] Capozza F, Combs TP, Cohen AW, Cho YR, Park SY, Schubert W, et al. Caveolin-3 knockout mice show increased adiposity and whole body insulin resistance, with ligand-induced insulin receptor instability in skeletal muscle. Am J Physiol Cell Physiol 2005;288:C1317–31.
[15] Oshikawa J, Otsu K, Toya Y, Tsunematsu T, Hankins R, Kawabe J, et al. Insulin resistance in skeletal muscles of caveolin-3-null mice. Proc Natl Acad Sci U S A 2004;101:12670–5.
[16] Mu P, Tan Z, Cui Y, Liu H, Xu X, Huang Q, et al. 17beta-Estradiol attenuates diet-induced insulin resistance and glucose intolerance through up-regulation of caveolin-3. Ir J Med Sci 2011;180:221–7.
[17] Bowers JL, Tyulmenkov VV, Jernigan SC, Klinge CM. Resveratrol acts as a mixed agonist/antagonist for estrogen receptors alpha and beta. Endocrinology 2000;141:3657–67.
[18] Bryant NJ, Govers R, James DE. Regulated transport of the glucose transporter GLUT4. Nat Rev Mol Cell Biol 2002;3:267–77.
[19] Shoelson SE, Lee J, Goldfine AB. Inflammation and insulin resistance. J Clin Invest 2006;116:1793–801.
[20] Cani PD, Amar J, Iglesias MA, Poggi M, Knauf C, Bastelica D, et al. Metabolic endotoxemia initiates obesity and insulin resistance. Diabetes 2007;56:1761–72.
[21] Ng SF, Lin RC, Laybutt DR, Barres R, Owens JA, Morris MJ. Chronic high-fat diet in fathers programs beta-cell dysfunction in female rat offspring. Nature 2010;467:963–6.
[22] Davies MJ, Baer DJ, Judd JT, Brown ED, Campbell WS, Taylor PR. Effects of moderate alcohol intake on fasting insulin and glucose concentrations and insulin sensitivity in postmenopausal women: a randomized controlled trial. JAMA 2002;287:2559–62.
[23] Juntunen KS, Laaksonen DE, Poutanen KS, Niskanen LK, Mykkanen HM. High-fiber rye bread and insulin secretion and sensitivity in healthy postmenopausal women. Am J Clin Nutr 2003;77:385–91.
[24] Barrett-Connor E, Schrott HG, Greendale G, Kritz-Silverstein D, Espeland MA, Stern MP, et al. Factors associated with glucose and insulin levels in healthy postmenopausal women. Diabetes Care 1996;19:333–40.
[25] Rachon D, Vortherms T, Seidlova-Wuttke D, Wuttke W. Effects of dietary equol on body weight gain, intra-abdominal fat accumulation, plasma lipids, and glucose tolerance in ovariectomized Sprague–Dawley rats. Menopause 2007;14:925–32.
[26] Brasnyo P, Molnar GA, Mohas M, Marko L, Laczy B, Cseh J, et al. Resveratrol improves insulin sensitivity, reduces oxidative stress and activates the Akt pathway in type 2 diabetic patients. Br J Nutr 2011:1–7.
[27] Lagouge M, Argmann C, Gerhart-Hines Z, Meziane H, Lerin C, Daussin F, et al. Resveratrol improves mitochondrial function and protects against metabolic disease by activating SIRT1 and PGC-1alpha. Cell 2006;127:1109–22.
[28] Barros RP, Machado UF, Gustafsson JA. Estrogen receptors: new players in diabetes mellitus. Trends Mol Med 2006;12:425–31.
[29] Le MC, Chu K, Hu M, Ortega CS, Simpson ER, Korach KS, et al. Estrogens protect pancreatic beta-cells from apoptosis and prevent insulin-deficient diabetes mellitus in mice. Proc Natl Acad Sci U S A 2006;103:9232–7.
[30] Foryst-Ludwig A, Kintscher U. Metabolic impact of estrogen signalling through ERalpha and ERbeta. J Steroid Biochem Mol Biol 2010;122:74–81.
[31] Rossi R, Origliani G, Modena MG. Transdermal 17-beta-estradiol and risk of developing type 2 diabetes in a population of healthy, nonobese postmenopausal women. Diabetes Care 2004;27:645–9.
[32] Gehm BD, McAndrews JM, Chien PY, Jameson JL. Resveratrol, a polyphenolic compound found in grapes and wine, is an agonist for the estrogen receptor. Proc Natl Acad Sci U S A 1997;94:14138–43.
[33] Prossnitz ER, Maggiolini M. Mechanisms of estrogen signaling and gene expression via GPR30. Mol Cell Endocrinol 2009;308:32–8.
[34] Riant E, Waget A, Cogo H, Arnal JF, Burcelin R, Gourdy P. Estrogens protect against high-fat diet-induced insulin resistance and glucose intolerance in mice. Endocrinology 2009;150:2109–17.

[35] Gorres BK, Bomhoff GL, Gupte AA, Geiger PC. Altered estrogen receptor expression in skeletal muscle and adipose tissue of female rats fed a high-fat diet. J Appl Physiol 2011;110:1046–53.
[36] Bickel PE. Lipid rafts and insulin signaling. Am J Physiol Endocrinol Metab 2002;282:E1–10.
[37] Ishikawa Y, Otsu K, Oshikawa J. Caveolin; different roles for insulin signal? Cell Signal 2005;17:1175–82.
[38] Karlsson M, Thorn H, Parpal S, Stralfors P, Gustavsson J. Insulin induces translocation of glucose transporter Glut-4 to plasma membrane caveolae in adipocytes. FASEB J 2002;16:249–51.
[39] Fecchi K, Volonte D, Hezel MP, Schmeck K, Galbiati F. Spatial and temporal regulation of GLUT4 translocation by flotillin-1 and caveolin-3 in skeletal muscle cells. FASEB J 2006;20:705–7.
[40] Oh YS, Cho KA, Ryu SJ, Khil LY, Jun HS, Yoon JW, et al. Regulation of insulin response in skeletal muscle cell by caveolin status. J Cell Biochem 2006;99: 747–58.
[41] Tsutsumi YM, Kawaraguchi Y, Horikawa YT, Niesman IR, Kidd MW, Chin-Lee B, et al. Role of caveolin-3 and glucose transporter-4 in isoflurane-induced delayed cardiac protection. Anesthesiology 2010;112: 1136–45.